Nonlinear gyrokinetic investigation of energetic particle driven geodesic acoustic modes

A. Biancalani[1], A. Bottino[1], N. Carlevaro[2], A. Di Siena[1], T. Görler[1], G. Montani[2], I. Novikau[1], and D. Zarzoso[3]

[1] *Max-Planck-Institut für Plasmaphysik, 85748 Garching, Germany*

[2] *ENEA C.R. Frascati - ENEA for EUROfusion, C.P. 65 - 00044 Frascati, Italy*

[3] *Aix-Marseille Université, PIIM, UMR 7345, 13397 Marseille, France*

Introduction

Zonal (i.e. axisymmetric) radial electric fields, associated to zonal poloidal flows, are known to develop in tokamak plasmas in the presence of turbulence. These zonal structures (ZS), are observed as zero frequency zonal flows (ZFZF), nearly stationary, or finite-frequency geodesic acoustic modes (GAM) [1, 2]. In the presence of energetic particles (EP), ZS can also be excited by inverse Landau damping, as EP-driven GAMs (EGAM) [3, 4, 5, 6, 7].

Here, we investigate the nonlinear dynamics of EGAMs, in the absence and in the presence of turbulence (see also Ref. [8]). The global gyrokinetic (GK) particle-in-cell code ORB5 is used. ORB5 was originally developed for ITG turbulence studies [9] and has more recently been extended to an electromagnetic multispecies version [10]. Here, we focus on linear and nonlinear electrostatic collisionless simulations, where kinetic electron effects are neglected.

Equilibrium

We use the same equil. as in Ref. [11]. The major radius is $R_0 = 1.0$ m, the minor radius is $a = 0.3125$ m, and the toroidal magnetic field at the axis is $B_0 = 1.9$ T. In Ref. [11], flat q, n, T profiles were considered. Here, the safety factor q is given by $q(\rho) = 1.74 + 1.3\rho^2$, with $q(\rho_r = 0.45) = 2$ at the reference radial position, corresponding to $s_r = \sqrt{\psi_r/\psi_{edge}} = 0.5$ (with ψ being the poloidal magnetic flux).

The ion and electron temperatures are equal, with $\rho^* = \rho_s/a = 0.00571$ and $\rho_s = c_s/\Omega_i$ being the sound Larmor radius (and with $c_s = \sqrt{T_e/m_i}$ being the sound velocity). Times are normalized to the ion cyclotron frequency Ω_i^{-1}. The temperature and density gradients normalized to the minor radius a are $\kappa_T = 3.7$ and $\kappa_n = 0.8$ at s=0.5.

The EP temperature profile is flat. The EP density will be considered either flat or with a gaussian shape centered at the reference radius s_r, with width $\delta/a = 0.1$, where a is the minor radius. In velocity space, the EP has a double bump-on-tail distribution in parallel velocity, as in Ref. [5, 11] with the same normalized temperature $\hat{T}_h = T_h/T_i = 1$ and normalized mean parallel

velocity $\bar{\zeta} = v_{||}/v_{ti} = 4$. Neumann and Dirichlet boundary conditions are imposed to the scalar potential, respectively at the inner and outer boundaries, $s = 0$ and $s = 1$.

Linear dynamics

For the equilibrium described in the previous section, and for a EP concentration of $n_{EP}/n_e = 0.08$, linear EGAMs simulations are performed. The linear frequency and growth rate of the EGAM for this EP concentration is $\omega_{EGAM} = 2.36 \cdot 10^{-3}\Omega_i = 0.94\,\omega_s = 4.3 \cdot 10^5$ rad/s, $\gamma_{EGAM} = 0.31 \cdot 10^{-3}\Omega_i = 0.12\,\omega_s = 0.56 \cdot 10^5$ rad/s.

A study of the radial structure is also performed with linear EGAM simulations in the absence of turbulence. Firstly, flat equilibrium radial profiles are considered for all species, like in the previous papers where EGAMs were studied with ORB5. The localized initial EGAM perturbation is observed to evolve in time, with decreasing value of k_r. On the contrary, when a radially localized EP density profile is introduced, the EGAM radial structure forms with characteristic width given by the EP profile (see Fig. 1). This behavior reflects the nature of EGAMs as forced modes, analogously to EPM for Alfvén-type modes.

When we introduce non-flat density and temperature profiles of the thermal ions and electrons, the EGAM remains localized near the mid-radius, with some changes in the structure and some oscillations of the position of the peak in time, between s=0.4 and s=0.6.

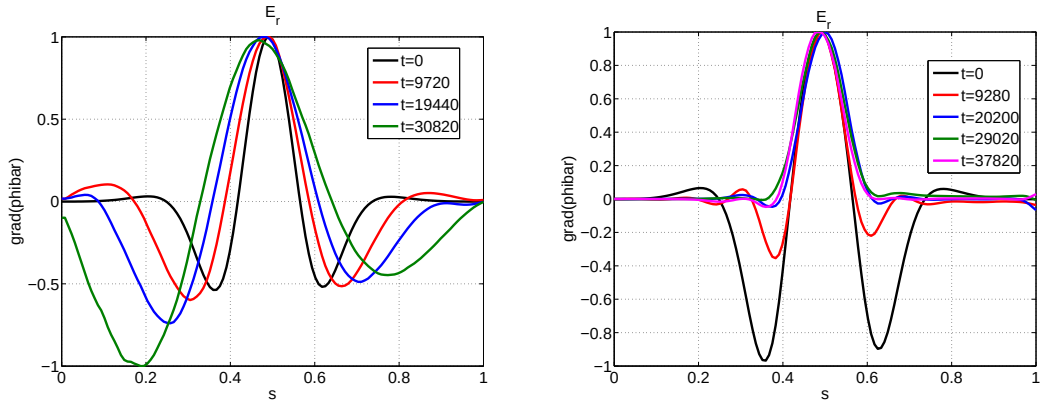

Figure 1: Radial structure of the linear EGAM electric field where all gradients are zero. On the left, a flat EP density profile is initialized. On the right, the localized EP density profile is used.

Nonlinear dynamics

In this section, we discuss the results of nonlinear simulations of EGAMs, where a radially localized EP density profile is initialized. A Krook-like operator acting as a heat source, modified to conserve particles, momentum and zonal flows [12], is used for the thermal ions, whose function is to maintain the ion temperature profile close to the original one. At the same time,

the Krook operator acts as noise control. No source is applied to the EP, because we want to investigate the effect of their nonlinear relaxation. For the selected EP density, i.e. $n_{EP}/n_e = 0.08$, the Krook operator used is found not to modify the EGAM linear growth rate and nonlinear saturation level.

Firstly, we investigate nonlinear EGAM simulations without turbulence (see Fig. 2-left), by filtering out all non-zonal perturbations at every time step. The EGAM is observed to grow linearly and then saturate, then entering a deep nonlinear phase where the mode initially decays, then oscillations in amplitude occur. Here, we are not interested in the deep nonlinear phase, but only in the level of the first saturation. Simulations with wave-particle + wave-wave nonlinearity are observed to saturate at a lower level with respect to simulations where the wave-particle nonlinearity only is switched on. Nevertheless, for the case of interest, the wave-particle nonlinearity is shown not to be negligible, and provide at least 50% of the saturation mechanism.

Secondly, we study the evolution in time of the zonal radial electric field in simulations of turbulence, without and with EP (see Fig. 2-right). In the simulation without EP, the ZS is observed to grow due to the nonlinear drive of the ITG turbulence, then saturate. In the simulation with EP, after the turbulence saturates, the EGAM starts growing on top of that, and saturates at a higher level. The growth rate of the ZS due to the turbulence is also higher when EP are present.

Comparisons with the GK codes GENE and GYSELA are also performed in the absence of turbulence. A good agreement of the linear and nonlinear dynamics is found, and a lower

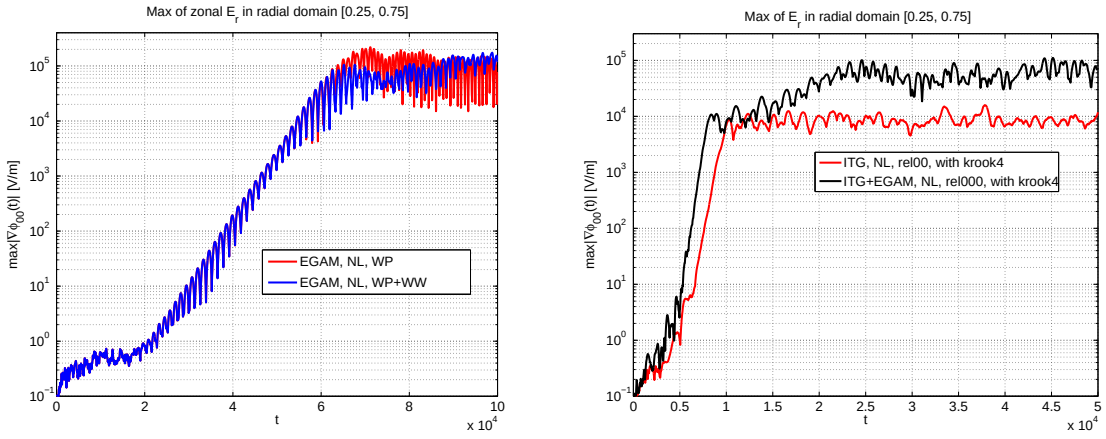

Figure 2: On the left, simulations of EGAMs without turbulence, with wave-particle nonlinearity only (red line) and wave-particle + wave-wave nonlinearity (blue line). The maximum value of the radial zonal electric field calculated in the radial domain $0.25 < s < 0.75$ is shown. On the right, simulations with turbulence, without EP (red line) and with EP (black line).

saturation level of EGAMs is confirmed when the wave-wave nonlinearity is switched on.

Conclusion and discussion

The linear and nonlinear dynamics of EGAMs is studied here, in the presence and absence of turbulence. Several nonlinear mechanisms are studied separately, and in particular the wave-particle and wave-wave nonlinearities. Comparing the first saturation level of the simulations with and without turbulence, we note that it does not depend on the presence of turbulence, for the case of interest, being $\delta E_{r,max} = 1.0 \cdot 10^5$ V/m (whereas it can change in the deep nonlinear phase). This means that the EGAM saturation mechanism for the case of interest is not the wave-wave nonlinearity between EGAM and ITG. We deduce that the EGAM saturates here for a combined effect of wave-particle nonlinearity (i.e. EP redistribution in velocity space, and resonance detuning due to the EGAM frequency chirping) and wave-wave nonlinearity (ZFZF and second-harmonic generation [7]). A comparison of the saturated level with the reduced model provided in Ref. [11] is also done. We find a good agreement of the order of magnitude of the saturated electric field.

Acknowledgments: Valuable discussions are acknowledged with F. Zonca, Z. Qiu, L. Villard, S. Brunner, A. Mishchenko and P. Lauber. This work has been carried out within the framework of the EUROfusion Consortium and has received funding from the Euratom research and training programme 2014-2018 under grant agreement No 633053. The views and opinions expressed herein do not necessarily reflect those of the European Commission. Simulations were performed on the Marconi supercomputer within the OrbZONE and ORBFAST projects.

References

[1] N. Winsor *et al.*, *Phys. Fluids* **11**, 2448, (1968)
[2] F. Zonca and L. Chen, *Europhys. Lett.* **83**, 35001 (2008)
[3] G. Y. Fu, *Phys. Rev. Letters* **101** (18), 185002 (2008)
[4] Z. Qiu, F. Zonca, and L. Chen *Plasma Phys. Control. Fusion* **52** (9), 095003 (2010)
[5] D. Zarzoso et al. *Phys. Plasmas* **19**, 022102-1 (2012)
[6] A. Di Siena, A. Biancalani, T. Görler, H. Doerk, I. Novikau, P. Lauber, A. Bottino, E. Poli, and the ASDEX Upgrade Team, submitted to *Nucl. Fusion* (2018)
[7] Z. Qiu, L. Chen and F. Zonca, "Kinetic theory of geodesic acoustic modes in toroidal plasmas: a brief review", accepted for publication in *Plasma Science and Tech.* (2018)
[8] D. Zarzoso, et al. *Phys. Rev. Letters* **110** (12), 125002 (2013)
[9] S. Jolliet, et al, *Comput. Phys. Commun.* **177**, 409 (2007).
[10] A. Bottino, et al *Plasma Phys. Controlled Fusion* **53**, 124027 (2011)
[11] A. Biancalani, et al *J. Plasma Phys.* **83** 725830602 (2017)
[12] B.F. McMillan, et al., *Phys Plasmas* **15**, 052308 (2008)